

FTIR Spectra of Ni (H-dmg)₂ Hydrogen Bonded With Six Dyes

Ketan Dodia¹, Vishal.R.Jain², Hitesh Parmar³, Sagar.M.Agravat¹ and A.T.Oza¹

¹Department of Physics, Sardar Patel University, Vallabh Vidyanagar – 388120 Gujarat, India.

²Navjevan Science College, Dahod, Gujarat, India.

³Arts Science And R.A.Patel Commerce College, Bhadran, Gujarat, India,

Abstract: Here the one-dimensional semiconductor namely bis (dimethylglyoximate) Ni^{II} is hydrogen bonded with 6 highly polarizable dyes which are Para red, Congo red, Direct red, Bismark brown, Evans blue and Trypan blue. The hydrogen bonding was verified with FTIR spectroscopy. FTIR spectra also reveal modification of absorption edges by exciton-phonon coupling there are threshold energies for the formation of free excitons and electron-hole pairs with phonon emissions in the intrinsic absorption edge spectrum. The remainder absorption at the value of the band gap is proportional to the exciton ionization energy in both direct and indirect excitons. This remainder absorption increases with the increase in the number of phonon bands in the absorption edge.

1 INTRODUCTION :

Bis (dimethylglyoximate) Ni^{II} [Ni^{II}(Hdmg)₂], is a one-dimensional system having metal chain in one direction of the crystals (1). This 1-d system is hydrogen bonded with 6 dyes which contain O-H or N-H group with O-H-O group of dioxime ligand. The hydrogen bonded complexes are studied with FTIR spectroscopy in the present work. Ni(Hdmg)₂ has electrical dc resistivity of 1010 ohm-cm at room temperature and band gap of 2.0 eV. It shows an allowed direct transition with an optical band gap of 1.9 eV. The resistivity drops at high pressure (2). The charge transfer complexes of Ni(Hdmg)₂ and Ni(Hdpg)₂-the phenyl analog were studied with IR spectroscopy (3).

2 EXPERIMENTAL DETAILS :

Ni(Hdmg)₂ was prepared by standard method using NiCl₂·6H₂O and dimethylglyoxime (6) as red precipitates. 6 dyes which are Congo red, Para red, Bismark brown, Direct red, Trypan blue and Evans blue were obtained from Aldrich chemical in pure forms. Ni(Hdmg)₂ and dyes were mixed in 1:4 proportions and grinded in agate mortar with pestle till color changed and till fine homogeneous powders were formed. The mixture were again grinded after mixing them further with dry spectrograde KBr powder. Round plates were prepared by compressing the powders in a die with manually operated compressing machine. The semitransparent plates were placed in spectrophotometer's dark chamber.

The spectra in the range 400-4000 cm⁻¹ were recorded using a GXFTIR single beam spectrophotometer manufactured by Perkin Elmer company in USA. It was having a resolution of 0.15 cm⁻¹, a scan range of 15600-30 cm⁻¹, a scan time of 20 scan sec⁻¹, and OPD velocity of 0-20 cm sec⁻¹. MIRTGS and FIRTGS detectors were used. A beam splitter of opt KBr type was used

having a range of 7800-370 cm^{-1} . The spectra were recorded in purge mode.

3 RESULTS AND DISCUSSION :

The molecular structures of $\text{Ni}(\text{Hdmg})_2$ and six dyes are shown (Figure 1). The hydrogen bonding occurs with O-H---O group of dioxime ligand surrounding the metal ion in the centre. These are bifurcated hydrogen bond because already one intramolecular O-H---O hydrogen bond exists.

The FTIR spectra of $\text{Ni}(\text{Hdmg})_2$ -Para red, $\text{Ni}(\text{Hdmg})_2$ -Congo red and $\text{Ni}(\text{Hdmg})_2$ -Direct red are shown (Figure 2). Similar spectra of $\text{Ni}(\text{Hdmg})_2$ -Bismark brown, $\text{Ni}(\text{Hdmg})_2$ -Evans blue and $\text{Ni}(\text{Hdmg})_2$ -Trypan blue are also shown (Figure 3).

The intrinsic absorption edge spectrum above 1700 cm^{-1} is analyzed by plotting $(\alpha h\nu)^2$, $(\alpha h\nu)^{1/2}$, $(\alpha h\nu)^{1/3}$, $(\alpha h\nu)^{2/3}$ vs $h\nu$ and finding the best fit. $(\alpha h\nu)^{1/3}$ vs $h\nu$ was found to be the best fit indicating $(\alpha h\nu) = A(h\nu - E_g)^3$ corresponding to forbidden indirect transition in all complexes except the Trypan blue complexes. In $\text{Ni}(\text{Hdmg})_2$ -Trypan blue, $(\alpha h\nu) = A(h\nu - E_g)^{1/2}$ an allowed direct transition was found to be the best fit. These best fits are shown (Figure 4). The absorption edge is modified by exciton-phonon coupling. There are threshold energies for the formation of excitons and electron-hole pairs with phonon emission. If the exciton-phonon coupling is strong, there are less number of phonon emissions. If this coupling is weak, there are large number of phonon emissions. Here there are only two pronounced phonon bands in Bismark brown complex and there are eight phonon bands in the case of Para red complex. Other cases are intermediate cases. The number of phonon bands vs

band gap is plotted. Again band gap is found to decrease for strong exciton-phonon coupling (Fig 5).

The excitonic threshold energies are observed in GaP (4,6), SiC (7) and CdTe (8) and absorption edges were found to be modified by exciton-phonon coupling. This coupling for direct excitons is discussed (8). Every atomic system has an infinite set of discrete energy levels corresponding to finite motion of the electron. When the potential energy of the interaction is normalized to be zero at infinity, the total energy of the electron is negative. For positive values of energy the electron is not bound to the ion and is moving freely. The energy spectrum of free motion is continuous. Overlapping transitions into discrete and continuous regions of the energy spectrum prevent the absorption coefficient from turning zero when $\hbar\omega = \Delta E_0 (E_g)$. The absorption spectrum of direct allowed interband transition is given by

$$\alpha = (2\pi e^2 / m_0^2 c \omega n) (2m_{\text{red}}^* / \hbar^2)^{3/2} \times |P_{\text{nn}}(0)|^2 (E_1^{\text{ex}})^{1/2} (e^2 / \sin h z) \quad (1)$$

$$\text{where } z = \pi (E_1^{\text{ex}} / \hbar\omega - \Delta E_0)^{1/2}$$

For $\hbar\omega \rightarrow \Delta E_0$ we obtain

$$\alpha(\Delta E_0) = (4\pi e^2 / m_0^2 c \omega n) (2m_{\text{red}}^* / \hbar^2)^{3/2} \times |P_{\text{nn}}(0)|^2 (E_1^{\text{ex}})^{1/2} \quad (2)$$

i.e. the greater the exciton ionization energy E_1^{ex} the greater is α at $\Delta E_0 (E_g)$. For $E_1^{\text{ex}} \rightarrow 0$, $\alpha(\Delta E_0) \rightarrow 0$. and α takes the form $\alpha \sim (\hbar\omega - \Delta E_0)^{1/2}$. For direct forbidden transitions the corrections obtained are similar. The theory of indirect exciton transitions has also been developed. There should be a well – defined long –

wave boundary of the fundamental band. Actually the long – wave edge of the fundamental absorption band is more or less spread out in the direction of $\hbar\omega < \Delta E_0$ (E_g). The equations (1) and (2) are applied to trypan blue complex where direct transition is observed.

The theory of light absorption resulting in interband transitions of electrons, coulomb interaction between electrons and holes created in the process of photon absorption is not taken into account. Coulomb attraction is instrumental in creating a bound electron-hole system, the exciton, which has a hydrogen-like discrete energy level systems $E_N^{ex} = E_c - (E_1^{ex}/N^2)$ below the bottom of the conduction band. The fundamental state of the exciton is below E_c by the amount

$$E_1^{ex} = (13.5/e^2)(m_{red}^*/m_0) \text{ eV}$$

In the course of direct interband transitions from the state $k=k_n$ a hole with wave vector $k_p = -k$ is created. since the exciton travels as a whole, it follows that the motion of the electron and the hole is correlated and that their relative velocity is zero. This is possible if the exciton springs from the transitions $k_n = k_p = 0$, i.e. if the transitions take place in the centre of the Brillouin zone or generally in the energy extrema. The range of states from which allowed electron transitions resulting in the generation of excitons are possible is quite narrow. This is the cause of formation of narrow absorption spectral bands adjoining the fundamental band from the long-wave side. The formation of narrow discrete absorption bands is not the only modification of the excitation states. The exciton states are also responsible for the modification of the intrinsic absorption band pattern.

The pattern of the intrinsic absorption band edge for the exciton-phonon interband transitions in many solids may be described by the Urbach equation valid for a wide range of α .

$$\alpha(\hbar\omega) = \alpha_0 e^{-[\sigma(\hbar\omega - E_0)/KBT]}$$

The parameter E_0 may be correlated with the energy maximum of the exciton absorption band. This parameter coincides with the value of the absorption coefficient in the maximum of the exciton band. σ is in range 1-3.

The theory of optical absorption by excitons was developed (9). Also the temperature dependence of the Urbach optical absorption edge was studied (10). A nearly universally observed feature of optical absorption spectra near band edges in crystalline and amorphous semiconductors is the Urbach-Martienssen absorption edge given by

$$\alpha(\omega) = \alpha_0 \exp\{[\hbar\omega - E_G(T)]/E_0(T)\}$$

Where $\hbar\omega$ is the photon energy and E_G and E_0 are temperature-dependent fitting parameters. E_0 is the width of the tail. E_G is comparable to the band gap energy. E_0 is given by

$$E_0 = [\delta \ln \alpha / \delta(\hbar\omega)]^{-1}$$

and it is in the range 10-100 meV for amorphous semiconductors. E_G and E_0 scales almost linearly. E_G decreases as E_0 increases. There is a linear scaling relation (Figure 6). This is also supported by theory (10).

The theory for indirect excitons coupled with phonons is also developed. The remainder absorption coefficient at $E = E_G$

remains finite and is proportional to the ionization energy of the exciton. Here the remainder absorption in percentage is plotted vs no. of phonon bands and vs band gap in eV (Figure 7).

As band gap increases, the remainder absorption at $h\nu=E_g$ decreases. When exciton-phonon coupling is strong, the remainder absorption at E_g is more. Since the remainder absorption at E_g is proportional to the ionization energy of exciton, this shows that the excitons with more ionization energy are strongly bound to phonons. Band gap is less when the exciton ionization energy is more.

4 CONCLUSION :

The FTIR spectra of $Ni(Hdmg)_2$ with 6 dyes which are Para red, Direct red, Congo red, Evans blue, Bismark brown and Trypan blue have been studied. The intrinsic absorption edge spectrum is modified with threshold energies of excitons by exciton-phonon coupling. The remainder absorption is found at E_g due to this coupling which is proportional to the ionization energy of exciton. Excitons with higher ionization energies are strongly bound to phonons than those with less ionization energy. Band gap reduces with increase in ionization energy of excitons.

CAPTIONS OF THE FIGURES :

Figure 1 Molecular structures of $Ni(Hdmg)_2$ and six dyes.

Figure 2 FTIR spectra of

- (a) $Ni(Hdmg)_2$ -Para red
- (b) $Ni(Hdmg)_2$ -Congo red and
- (c) $Ni(Hdmg)_2$ -Direct red

Figure 3 FTIR spectra of

- (a) $Ni(Hdmg)_2$ -Bismark brown
- (b) $Ni(Hdmg)_2$ -Evans blue and
- (c) $Ni(Hdmg)_2$ -Trypan blue.

Figure 4 $(\alpha h\nu)^{1/3}$ vs $h\nu$ for

- (a) $Ni(Hdmg)_2$ -Para red
- (b) $Ni(Hdmg)_2$ -Congo red
- (c) $Ni(Hdmg)_2$ -Direct red
- (d) $Ni(Hdmg)_2$ -Bismark brown
- (e) $Ni(Hdmg)_2$ -Evans blue and $(\alpha h\nu)^2$ vs $h\nu$ for
- (f) $Ni(Hdmg)_2$ -Trypan blue.

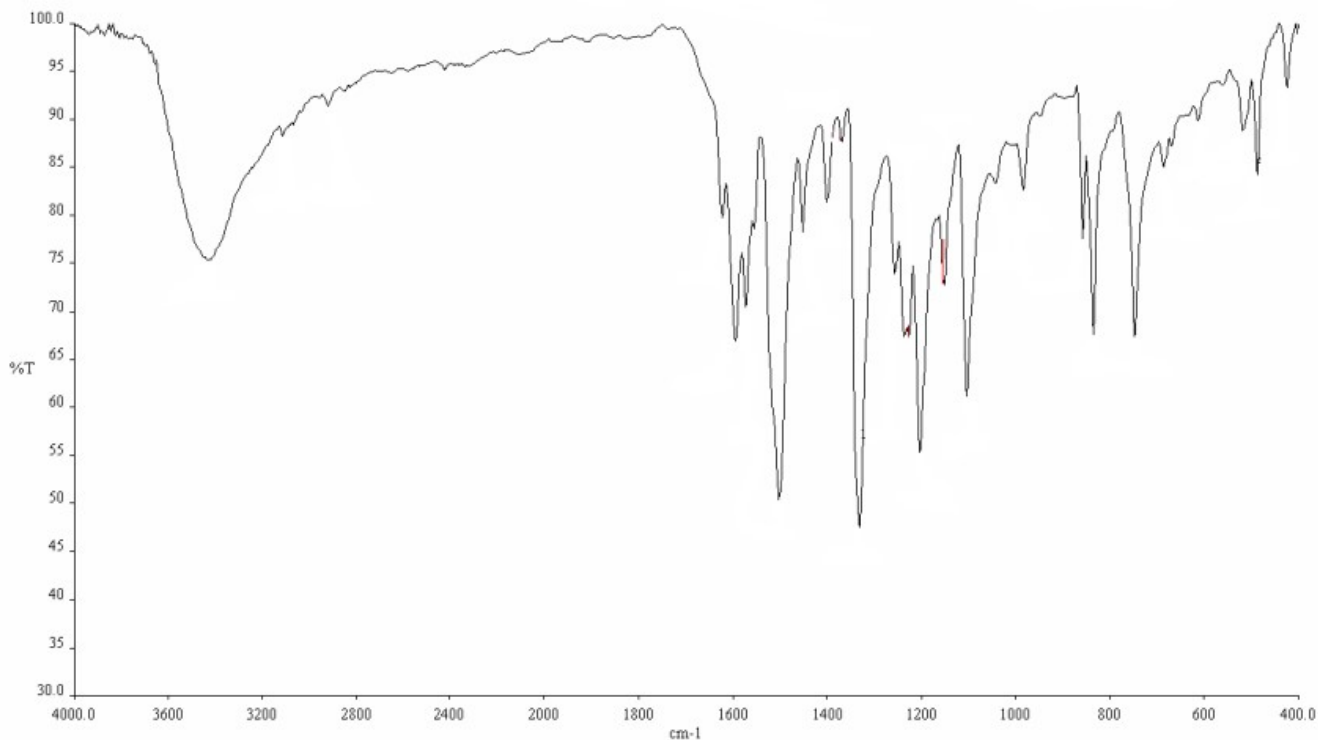
Figure 5 Number of phonon bands vs band gap (eV).

Figure 6 (a) Band tailing analysis and focal point.

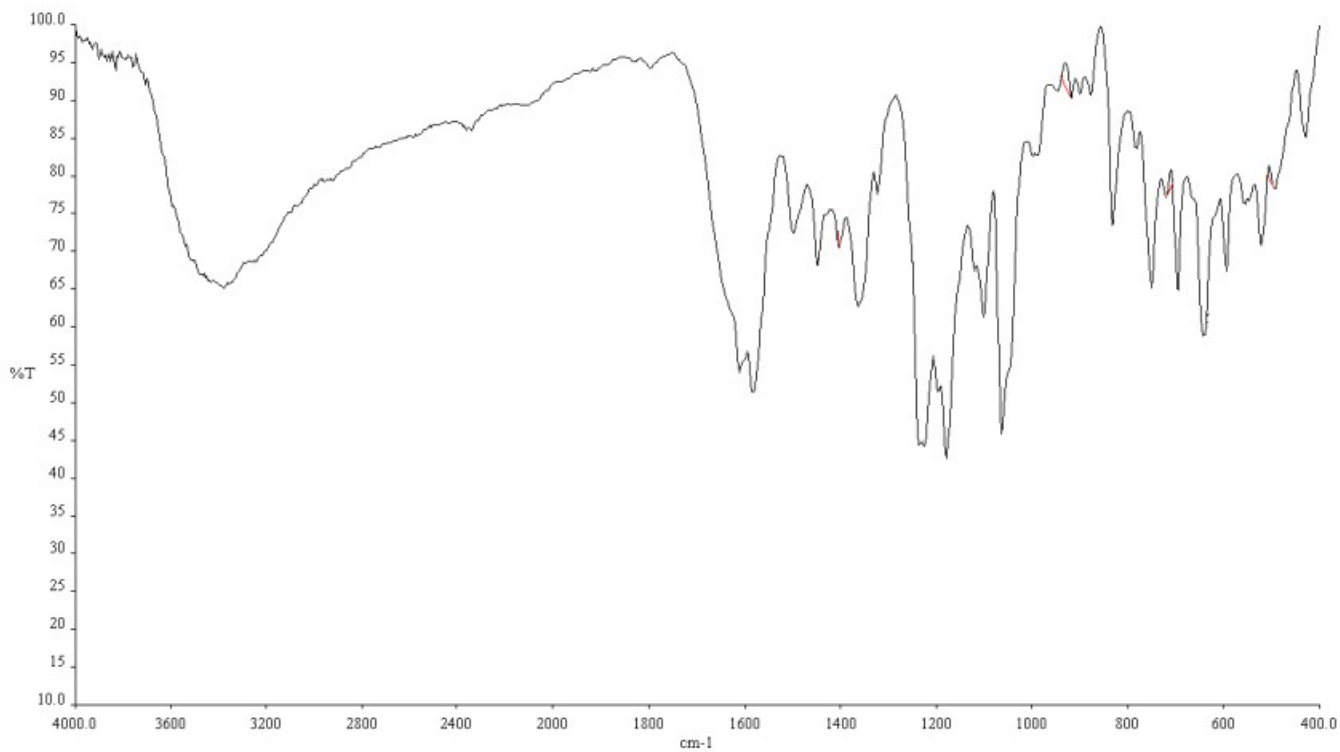
- (b) E_g vs E_0 i.e. band gap vs width of the tail.

Figure 7 (a) Number of phonon band vs remainder absorption at E_g .

- (b) Band gap (eV) vs remainder absorption at E_g .



(Figure-2a)



(Figure-2b)

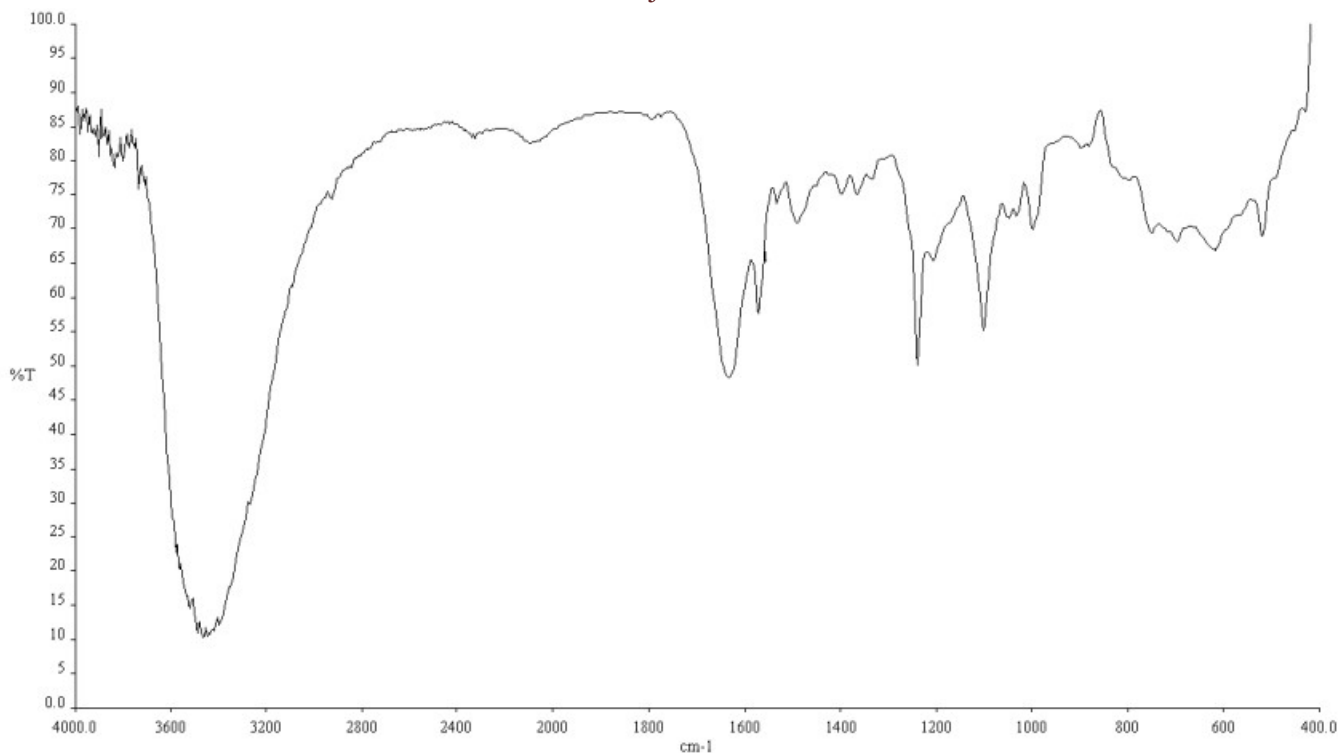


(Figure-2c)

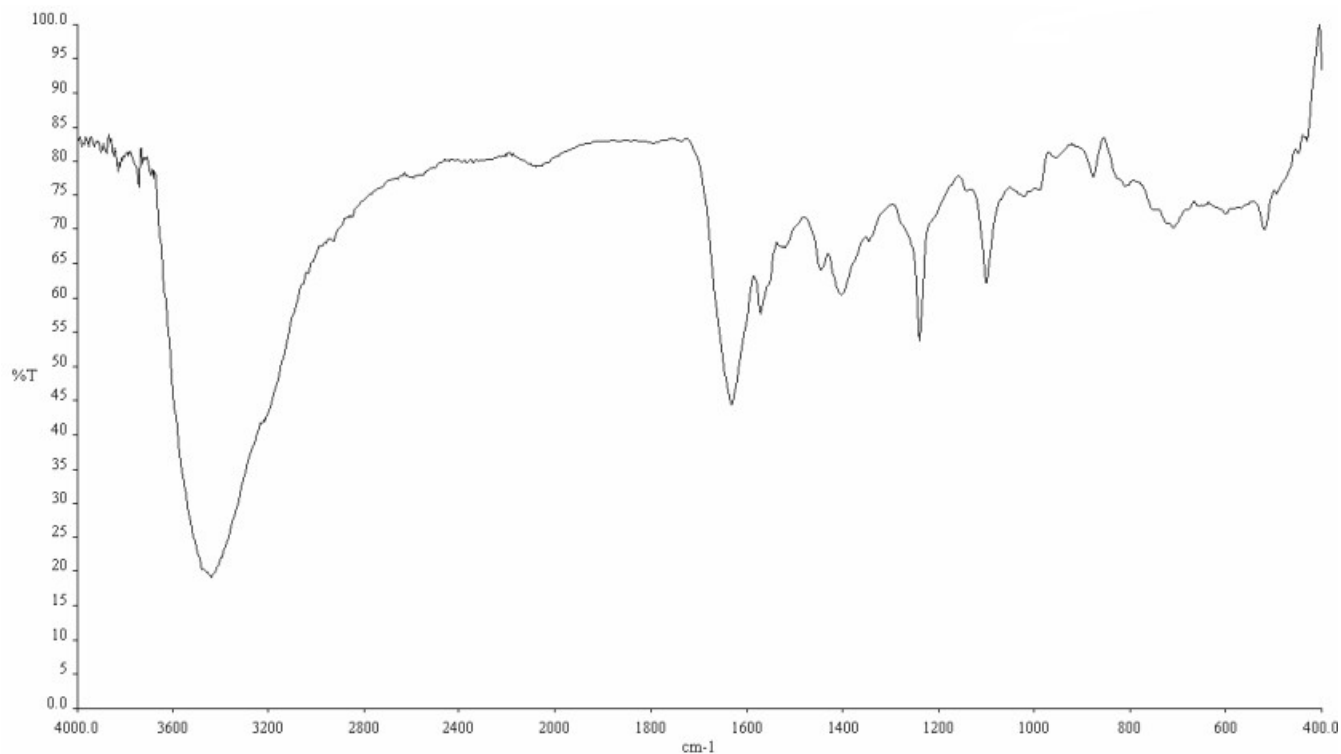


(Figure-3a)

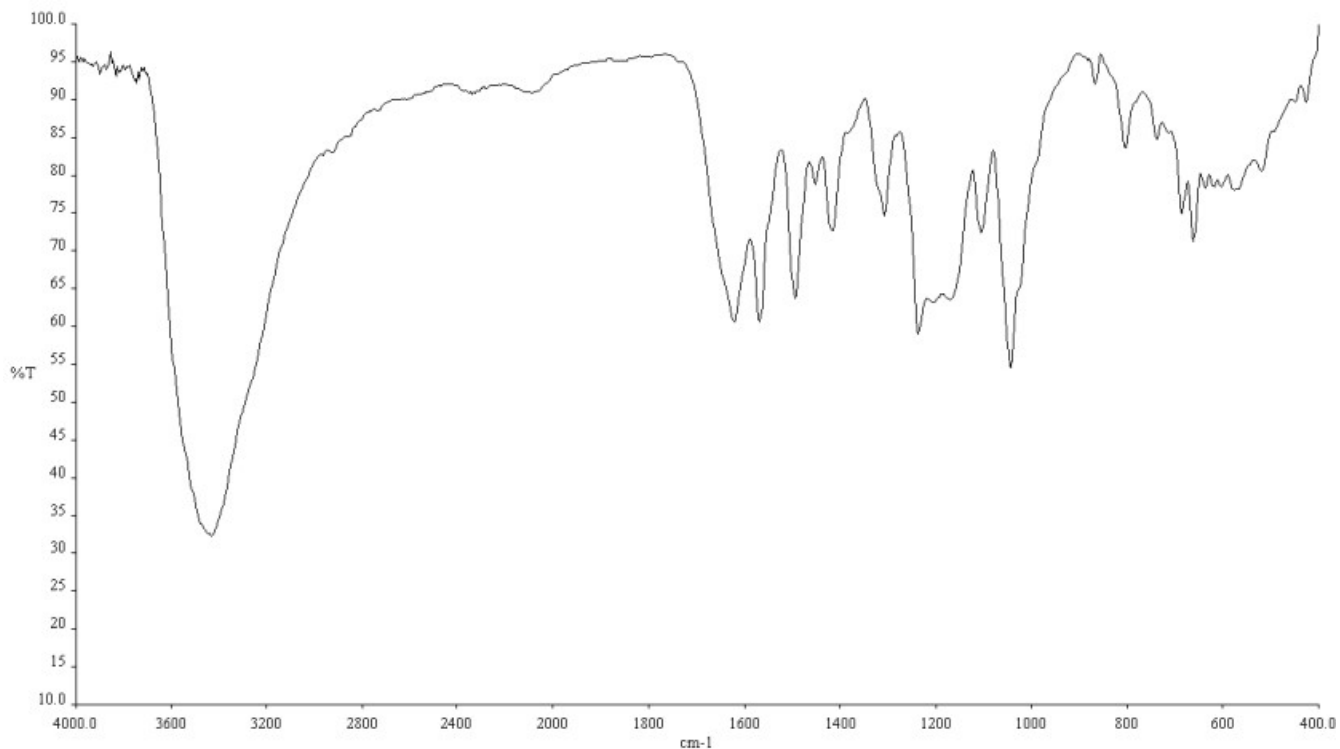


(Figure-3b)

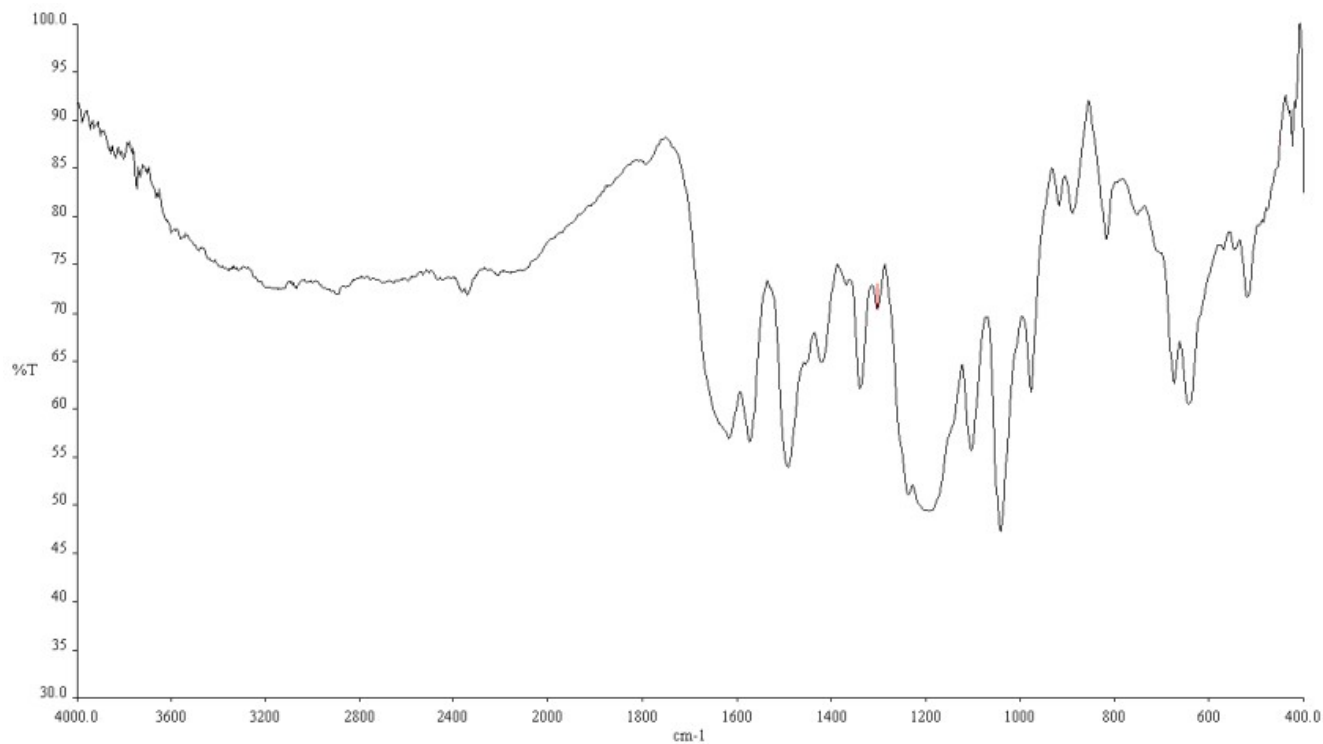


(Figure-3c)

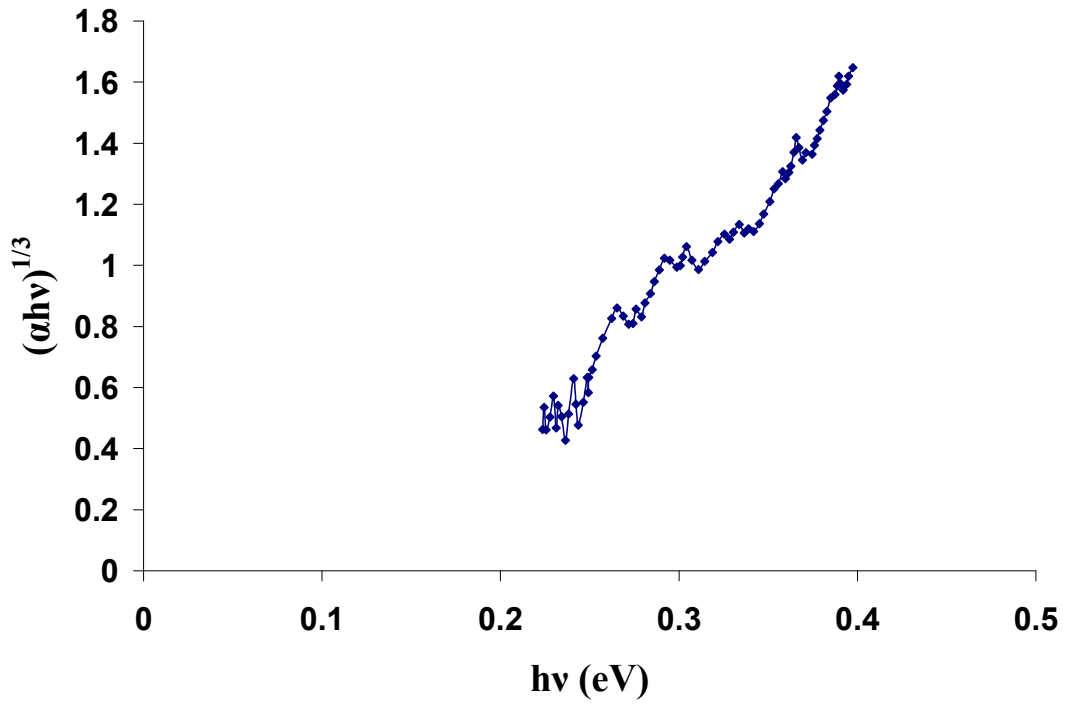


(Figure-4a)

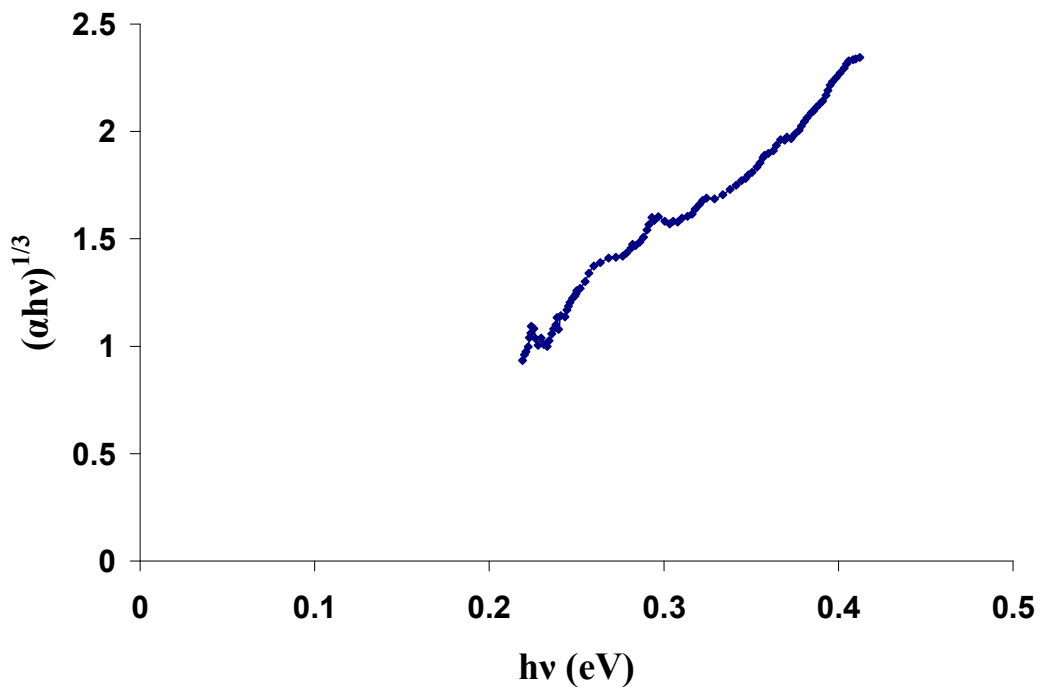


(Figure-4b)

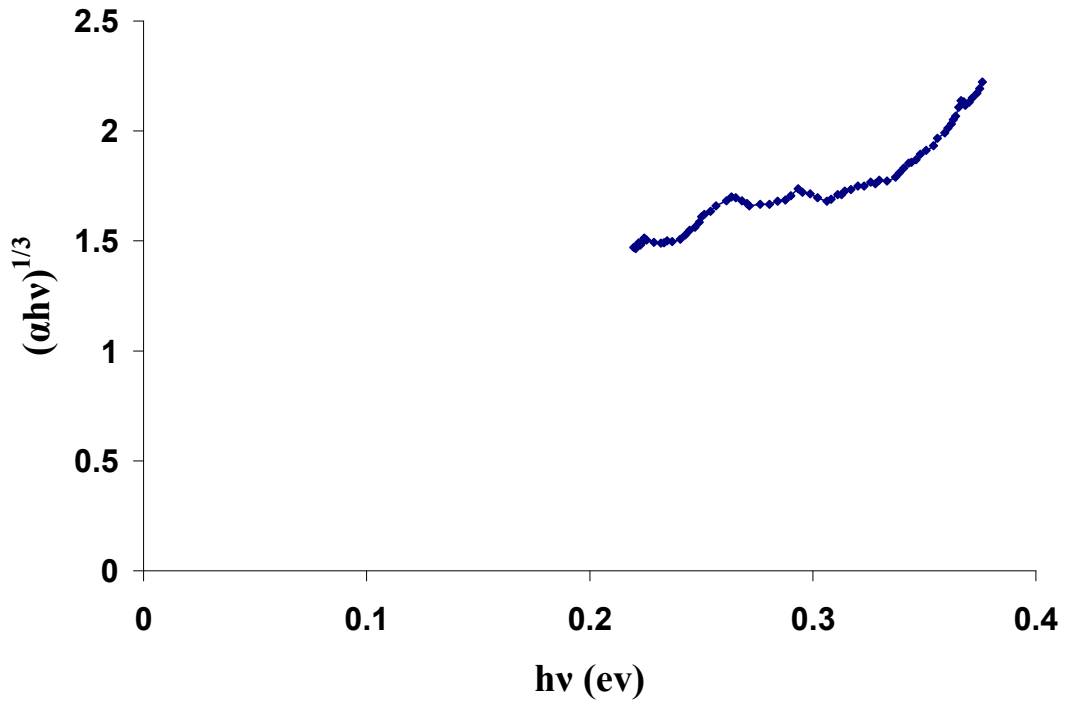


(Figure-4c)

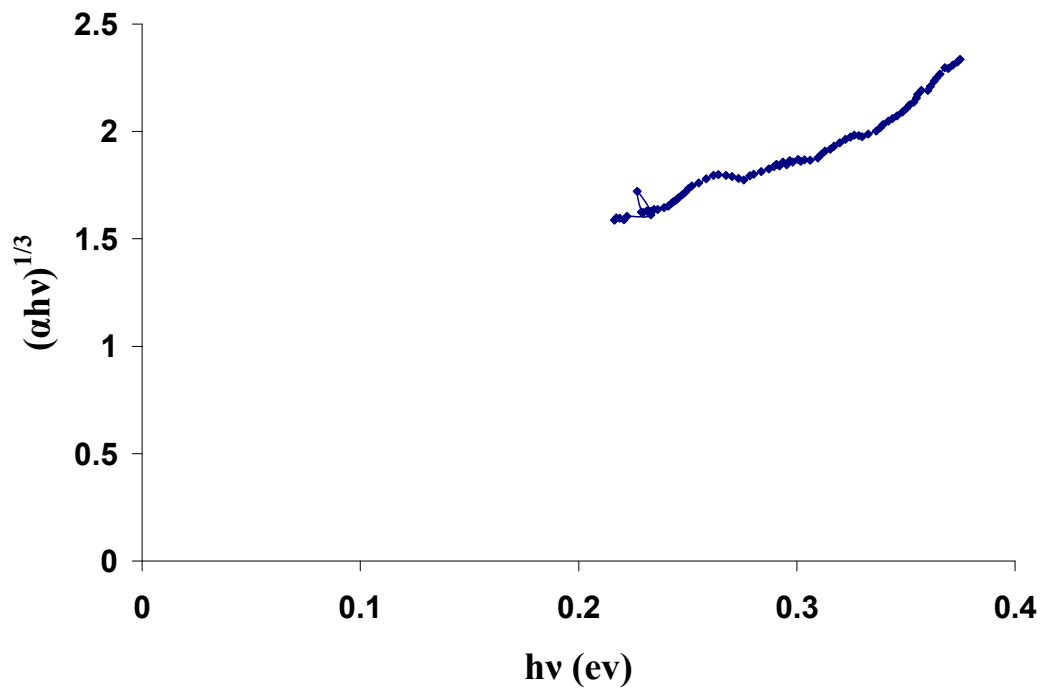


(Figure-4d)

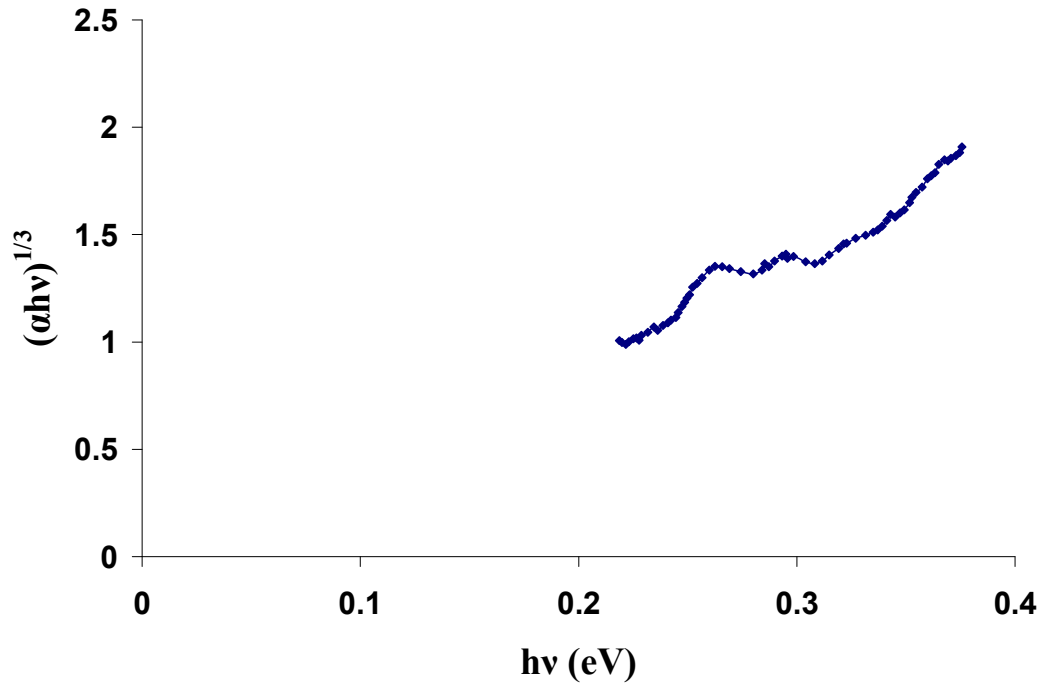


(Figure-4e)

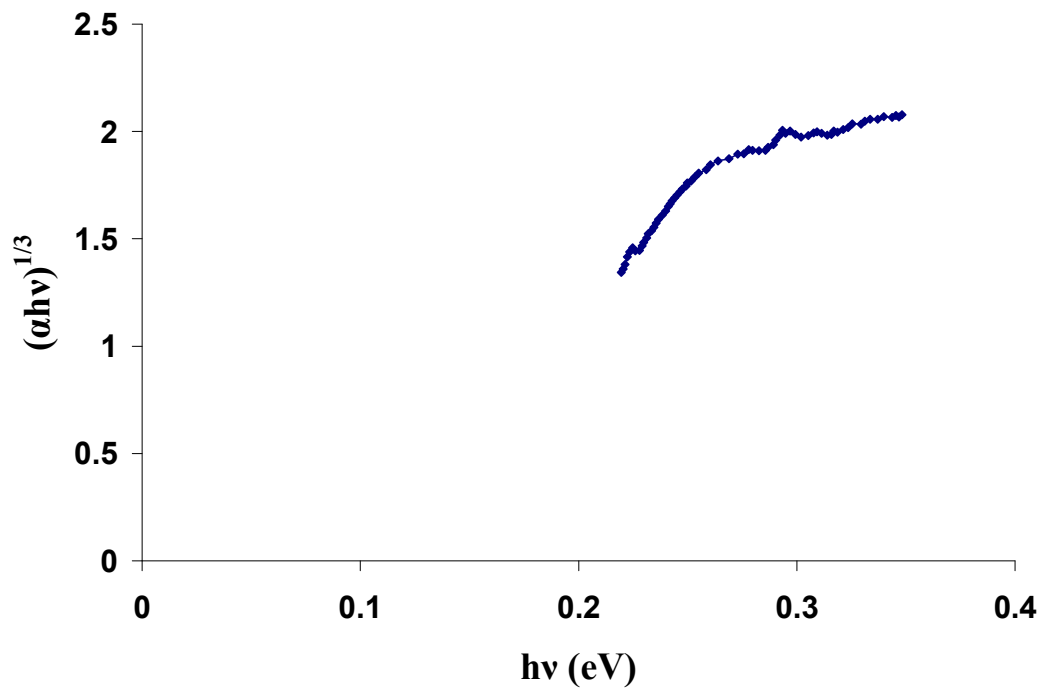


(Figure-4f)

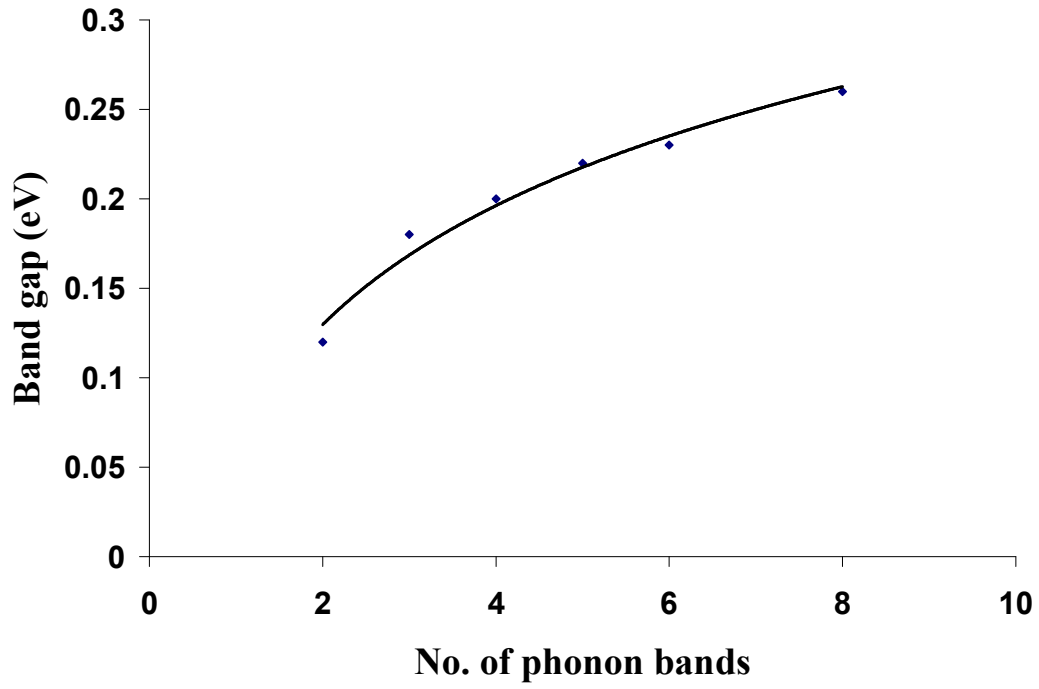


(Figure-5)

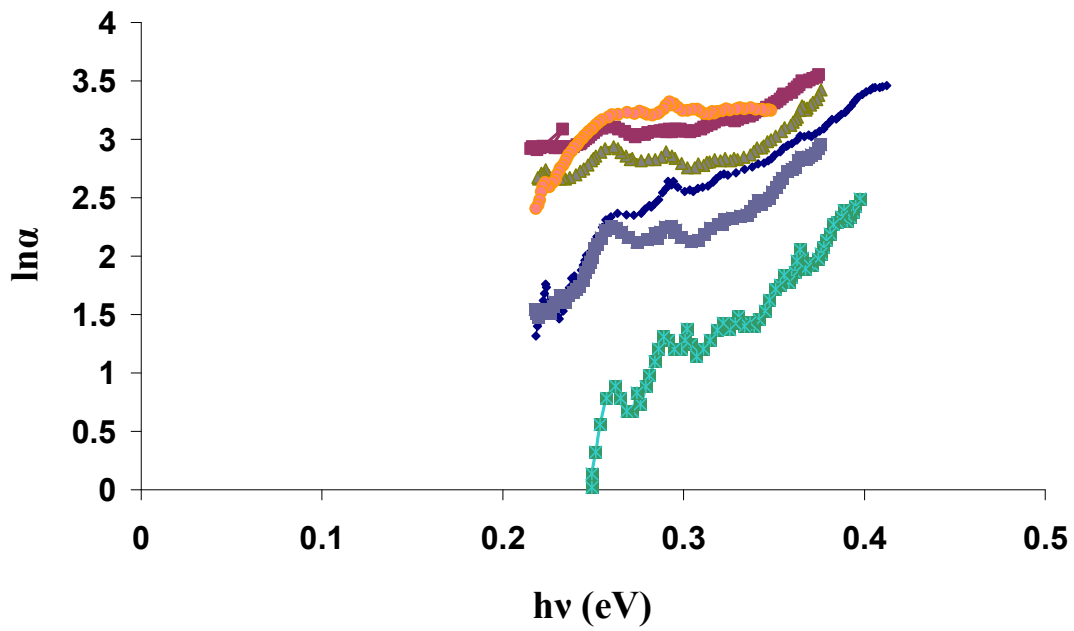


(Figure-6a)

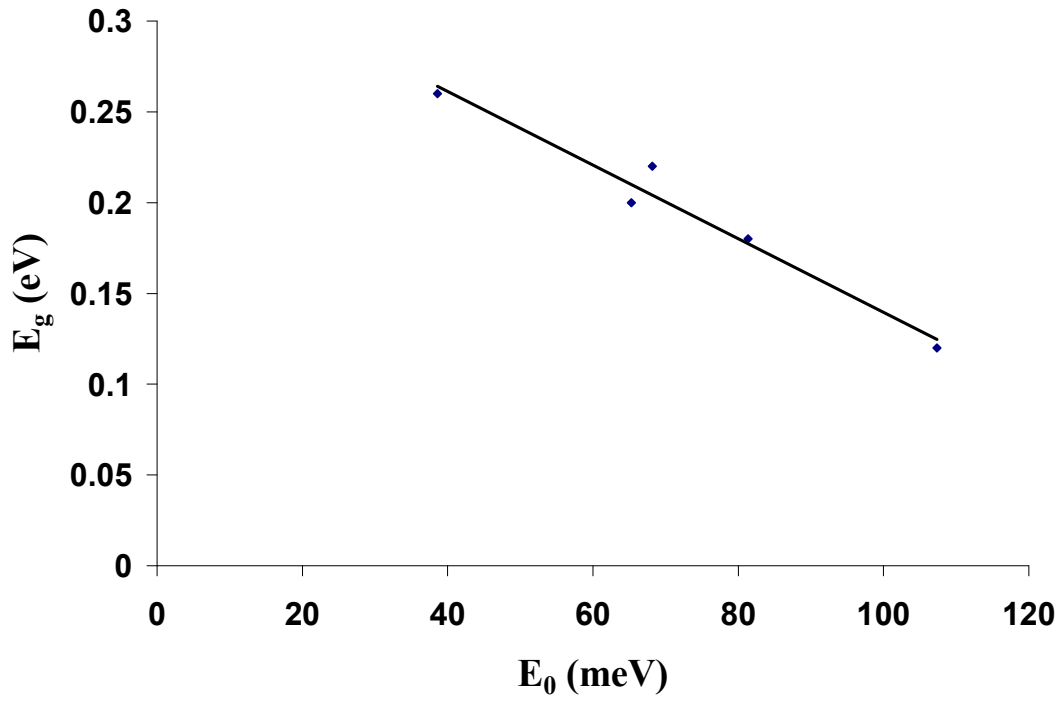


(Figure-6b)

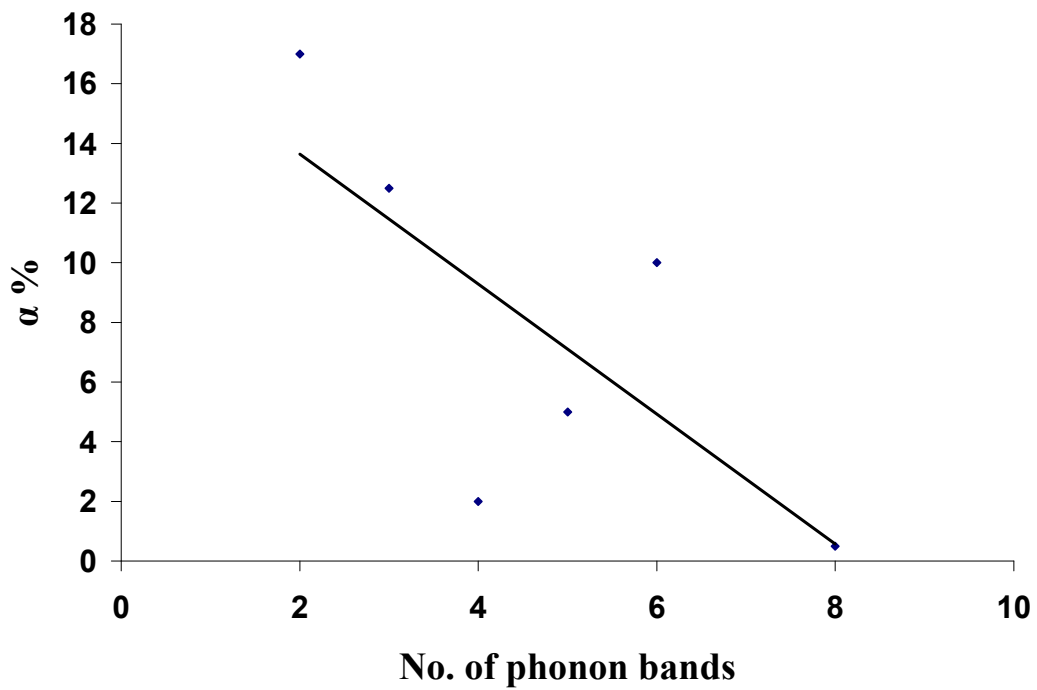


(Figure-7a)

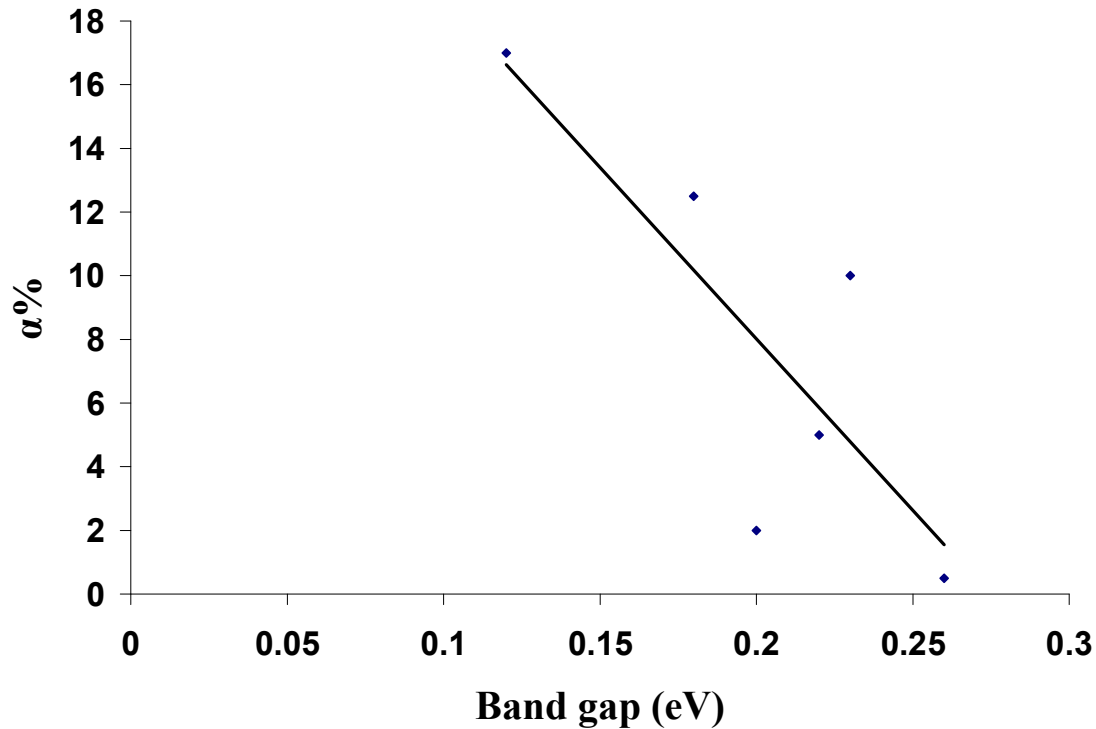


(Figure-7b)

REFERENCES :

1. L.E.Godycki and R.E. Rundle, Acta cryst,6,487,1953.
2. A.T.Oza, Czech.J.Phys.,43,821,1993.
3. R.G.Patel and A.T.Oza,Ind.J.Phys.,74B,31,2000.
4. J.I.Pankove,Optical Processes in semiconductors,Prentice-Hall Inc.,Englewood Cliffs,New Jersey,1971(p.59).
5. M.Gershenson, D.G.Thomas and R.E.Dietz, Proc.Int.Conf. on semiconductor Physics, Exeter, Inst. of Phys. and Phys.Soc.London,1962 (p.752).
6. P.J.Dean and D.G.Thomas,Phys.Rev.150,690,1966.
7. A.P.Hrokhmal, Semiconductors,37,279,2003.
8. P.S.Kireev, Semiconductor Physics, Mir Publishers, Moscow,1974 (P.553).
9. R.J.Elliott, Phys.Rev.108,1384,1957.
10. C.H.Grain and Sajeev John, Phys.Rev,B,39,1149,1989.